From biomass to diesel additives: Hydrogenation of cyclopentanone-furfural aldol condensation adducts

Jennifer Cueto, Paula Rapado, Laura Faba, Eva Díaz, Salvador Ordóñez*

Catalysis, Reactors and Control Research Group (CRC), Dept. of Chemical and Environmental Engineering, University of Oviedo, Oviedo 33006, Spain

* email: sordonez@uniovi.es; Tel.: +34 985 103 437; Fax: +34 985 103 434

ABSTRACT

The hydrogenation of furfural-cyclopentanone (C15) condensation adduct is studied in this work. Three different metals (Pt, Pd, Ni) supported on two materials (Al_2O_3 and Nb_2O_5) were compared, highlighting the good results obtained with Pd/Al_2O_3. The kinetic analysis of the reaction results suggests a parallel route in which the hydrogenation of cyclic unsaturation can occur simultaneously with the hydrogenation of aliphatic C=C. A key role of metal dispersion is discarded, concluding that this reaction is selective to the presence of Pd nanoparticles with a synergetic effect with the Al_2O_3 support, mainly due to the presence of strong acidic sites. Different organic solvents have been tested, including protic, polar and apolar ones. The best results are obtained with hexane and butanol, combining the absence of competitive adsorption and reactant solvation. At optimum conditions, more than 75 % of yield to the fully hydrogenated molecules were obtained in less than two hours, obtaining a mixture with good properties as a fuel additive.

KEYWORDS: saturated organics, palladium, hexane, 1-butanol, platinum

INTRODUCTION

The catalytic conversion of biomass to chemicals and liquid fuels is of the highest interest for the scientific community as a very promising route to replace fossil resources [1]. Hemicellulose and cellulose hydrolysis under acidic conditions (producing the subsequent dehydration of reduced sugars) allows obtaining several platform molecules with fewer oxygen atoms than the original sugar monomers [2]. These compounds (5-hydroxymethylfurfural – HMF-, furfural, cyclopentanone, levulinic acid, etc.) are included in the list of the most relevant bioplatform molecules. They can be used as chemical intermediates of fuel precursors and additives [3, 4]. In most cases, the upgrading of these compounds involves an intermediate step to create C-C bonds, increasing the carbon chain length, the aldol condensation being the most typical reaction proposed to this aim [5-7].

The aldol condensation between cyclic aldehydes (furfural and 5-HMF) and cyclopentanone or acetone as linking molecules allows obtaining C8-C17 adducts, being the optimum range defined for gasoline and diesel fuels and additives [8,9]. These reactions have been deeply studied, by both basic and acid catalysis, obtaining high activities and selectivities at mild conditions. Thus, basic catalysts such as mixed oxides [8,10,11], zirconium carbonates [12] and functionalized zeolites [13], among others, have been proposed in the literature. Concerning the acid mechanism, promising results are reported with different modified zeolites, including metal exchanges (Sn, K, etc.) to enhance their acidic properties [14,15]. In the last years, alternative routes have been also explored, such as photocatalysis and photo-electrocatalysis [16], but these preliminary studies only consider small molecules, such as butanol, as the reactant.

Compounds obtained by aldol condensation of cyclic aldehydes with linking molecules (C8-C17 adducts) still contain unsaturations and oxygen atoms, functional groups that must be totally or partially removed to guarantee high quality in the final product [17]. The first approaches proposed hydrodeoxygenation, intending to the corresponding alkanes from these adducts; therefore, producing the saturation of double bonds and the selective removal of oxygen from the molecule without cleaving the C-C bonds [18]. This reaction is catalysed by bifunctional catalysts

involving metals nanoparticles (Pd, Pt, Ru, Ni, Cu) supported on different materials, such as activated carbon, alumina, zeolites, titania and niobium-based solid acids [19-22]. However, the very low selectivity to the total hydrodeoxigenated compounds at reaction conditions consistent with the Principles of Green Chemistry (>500 K required to see the first traces) and the high excess of hydrogen required to obtain significant productivity (with the subsequent security issues) discourages this alternative. This fact is even more relevant when using furfural as a precursor since its hydrogenation produces the tetrahydrofuran (THF) cycle, a very stable molecule that requires severe conditions to be broken.

An intermediate approach consists of hydrogenating all the C-C double-bound without removing the oxygen atoms or opening the cycles [23-25]. According to the literature, resulting compounds have physical properties consistent with the diesel fuel requirements (cetane number, freezing point, kinematic viscosity, etc.) [25]. Thus, comparing the condensated adduct with the corresponding hydrogenated adduct (without cycle opening nor oxygen removal) the kinematic viscosity decreases by almost 60 %, the freezing point decreases from room temperature (20-30ºC) to less than -40ºC, and the lubricity increases from 160 mm to 220 mm. All these improvements are accomplished working at milder conditions than deep hydrodeoxygenation. Thus, the balance quality *vs.* economy of this alternative is considered positive. However, there is a lack of studies about this approach, without systematic analyses of reaction conditions and catalytic activity to optimize the stable and selective hydrogenation (and not hydrodeoxygenation) of biomass-derived aldol condensations.

In this context, we study in this paper the selective hydrogenation of furfural-cyclopentanone adduct (C15, F_2C), analysing the activity of several bifunctional catalysts, combining different metal nanoparticles (Pd, Pt, Ni) supported on two different acidic materials (Al_2O_3 and Nb_2O_5). Alumina is well-known support for these reactions, whereas niobium oxide is a promising material for deoxygenation reactions that highlights by its compatibility with water as solvent [17,26]. As to the metals chosen for this study, the high hydrogenation activity of Pd and Pt nanoparticles in hydrogenation is well known [19, 27]. Ni activity is also quite promising in this

type of reactions [28] and good behaviour of this metal could imply significant improvements from the economical point of view of a future industrial approach. Considering the key role of the solvent in these processes [21], different solvents and solvent mixtures have been also tested. Results are compared in terms of reaction kinetics and stability. Best results are considering for a preliminary approach to continuous configuration, in a fix-bed reactor.

MATERIALS AND METHODS

Catalysts preparation

The catalyst supports, Nb_2O_5 and γ-Al_2O_3, were kindly supplied by CBMM and BASF, respectively. An initial pretreatment under airflow has been done previous the metal impregnation with a ramping rate of 5 $K \cdot min^{-1}$. The final temperature reached as well as the time for holding it depends on the material: 723 K and 2 h for Nb_2O_5 and, 823 K and 4 h for Al_2O_3. Incipient wetness impregnation was selected as the technique to incorporate the metal into the catalyst surface. The precursors used were $Ni(NO_3)_2 \cdot 6H_2O$ (Sigma Aldrich, 99.99 %), $Pt(NH_3)_4(NO_3)_2$ (Sigma Aldrich, 99.995%) and $Pd(NH_3)_4(NO_3)_2$ (Sigma Aldrich, 99.995%). The aqueous solution of the precursors to obtain the desired metal loading (0.5 wt.%) was added drop-wise on 2 g of pretreated support. The resulting materials were dried at 383 K for 24 h before treating it, following the same procedure described for the supports. After this, the catalysts were exposed under 10 vol.% H_2/Ar and heated from room temperature to 473, 523, 693 and 723 K for Pd and Pt over Al_2O_3 [19], Pd and Pt over Nb_2O_5 [29], Ni/Al_2O_3 [30,31] and Ni/Nb_2O_5 [32], respectively. Pd/Al_2O_3 with 0.5 wt.% and 0.5 % Pt/Al_2O_3 were provided by BASF and only the reducing treatment was performed to ensure that all the metals were in the reduced state.

Catalysts characterization

The acidity of these catalysts was measured by temperature-programmed desorption (TPD) of NH_3 (NH_3-TPD) using a Micromeritics TPD/TPR 2900. NH_3 signal evolution was measured with

Pfeiffer Vacuum Omnistar Quadrupole Mass Spectrometer. Samples (20 mg) were pretreated before each analysis, being heated to 383 K in helium flow (20 mL·min^{-1}) for 1 h to remove any physisorbed compound from the surface. After, the catalytic surface was saturated in NH_3 flow (2.5 % NH_3/He, 20 mL·min^{-1}) at room temperature for 15 min. An intermediate stage of stabilization under helium flow was required to prevent signals related to oversaturation. Then, desorption of NH_3 was monitored, being flushed with helium (20 mL·min^{-1}) from room temperature to the maximum preparation temperature with a ramp of 5 K·min^{-1}.

Morphological-properties of these materials (surface area, pore diameter and total pore volumes) were determined by nitrogen physisorption at 77 K using an ASAP 2020 (Micromeritics) static volumetric apparatus after the corresponding degasification step.

The metal loading of the catalysts was determined by inductively coupled plasma mass spectrometry (ICP-MS) using an Agilent 7700x ICP-spectrometer. The samples were previously digested with HNO_3, diluted with deionized water, and analysed in the spectrometer.

The metal particle morphology and size distributions were identified by transmission electron microscopy (TEM) using a MET JEOL-2000 EX-II microscope. After measuring the size of more than 100 particles, the metal dispersion "D" is calculated according to the following equation:

$$D(\%) = \frac{6 \cdot \frac{v_m}{a_m}}{< d_p >} \cdot 100$$

Where "v_m" and "a_m" are the volume and surface of the metal particles, values calculate as a function of the atomic radius of each element and measured in cubic and square Armstrong's, respectively; "$<d_p>$" is the average particle diameter, measured in nanometers.

Reaction studies

C15 hydrogenation was carried out in a stirred batch autoclave reactor (0.5 L, Autoclave Engineers Eze Seal) equipped with a backpressure regulator and proportional-integral-derivative temperature controller. The system was loaded with the catalyst (0.1 or 1 g, 50-80 μm) and 0.25 L

of a solution that contains 3.5 $g \cdot L^{-1}$ of C15 and the corresponding solvent (hexane, heptane, acetone, 1-butanol, ethanol or 1:2 v/v of water/ethanol mixture). The reactant has been synthesized in the lab by the aldol condensation between cyclopentanone and furfural [8,10], being recovered as the solid obtained in this reaction. According to the analyses, this solid contains more than 95 % of C15 adduct, since it is the most insoluble product of the reaction. This residual composition (lower than 5 %) corresponds to C10 adduct (the first compound obtained in the cyclopentanone-furfural condensation). Although the hydrogenation of this compound would take place under similar reaction conditions, these compounds were not considered in the analysis to prevent interferences in the discussion. The stirring was 1000 rpm and the temperature was fixed at 493 K. The air was removed by pressurizing the system with nitrogen for three times previously hydrogen pressurization (25 bar at room temperature and, approximately 55 bar at 493 K). Once the operating conditions were achieved, samples were taken directly from the sample port to follow the evolution of reactant and products concentration. They were analyzed by gas chromatography (GC) in a Shimadzu GC-2010 equipped with a flame ionization detector (FID) detector, using a 30 m long CP-Sil 8 CB capillary column (30 m length, 0.25 mm internal diameter, following the temperature and flow programs detailed in the Supplementary Information (Table S1 and S2)). Peak assignment was performed by gas chromatography coupled to a mass spectrometer detector (GC-MS) in a Shimadzu GC/MS QP2010 Plus Instrument, using a TRB-5MS capillary column. The calibration of intermediates and products was carried out using the Response Factor Method according to the procedure proposed by Scanlon and Willis [33], since they are not commercially available, using the C15 experimental calibration as the basis. Once the concentration of each compound was calculated, the evolution of the reaction was studied considering conversion (x), atomic yield (ψ), selectivity (φ) and carbon balance closure (C.B.) concepts, according to the following expressions:

$$x = \frac{C_{C15,0} - C_{C15,t}}{C_{C15,0}} \cdot 100$$

$$\Psi = \frac{C_{i,t}}{C_{C15,0}} \cdot 100$$

$$\varphi = \frac{C_{i,t}}{\sum C_{i,t}} \cdot 100$$

$$C.B. = \frac{\sum C_{i,t} + C_{C15,t}}{C_{C15,0}} \cdot 100$$

Where $C_{C15,0}$ is the initial concentration of the reactant; $C_{C15,t}$ is the reactant concentration at a defined time, as well as $C_{i,t}$ is the concentration of a particular intermediate or final product.

RESULTS AND DISCUSSION

Metal and support influence

First experiments were carried out in binary system water:ethanol (2:1) with 3.5 $g \cdot L^{-1}$ of the C15 sample obtained in our previous work [10], at 493 K. As it was experimentally corroborated before each experiment, and according to the literature [34], this concentration is below the solubility limit of this compound in this system. In fact, the ratio of ethanol to water was optimized in previous work, being the equilibrium point between condensation activity (water) and products solubilisation (organic solvent) [10]. Thus, this configuration is chosen to evaluate an eventual one-pot process, involving condensation and hydrogenation steps as one reaction. The screening of several bifunctional catalysts was studied, combining three different metals (Pd, Pt and Ni) with two supports (Al_2O_3 and Nb_2O_5). All these catalysts have a theoretical metal loading of 0.5 %. A very good correspondence between theoretical and measured values was observed (ICP-MS analyses), as is shown in **Table 1**. This good correspondence could be anticipated, considering the preparation method (dry impregnation). The low metal loading guarantees small nanoparticles (lower than 10 nm in all the cases, according to TEM results shown in Table 1, detailed in Fig. S1). These small sizes enhance the metal activity required to saturate the C=C bonds. In addition, it minimizes the blockage of acidic sites of these supports, mainly required to guarantee optimum adsorption of the reactant and intermediates on the catalytic surface and to promote the hydrogenation of C=O unsaturations and the subsequent oxygen removal by dehydration. This is a key point since there is a general agreement in the literature about the

limiting character of this step in the whole process [24,35]. The influence of metal deposition on the catalytic acidity is clearly demonstrated comparing the different acid sites concentration and distribution of those catalysts prepared with the same support, i.e., the same original acidity, see Table 1. All the reactions were carried out at 25 bar of hydrogen as initial pressure and 493 K (55 bar).

Table 1: Morphological, surface and physic-chemical properties of catalysts used in this work.

	N_2 physisorption			Acidity (µmol/g)				ICP	TEM	
Catalyst	**S BET (m^2/g)**	**d_p (nm)**	**V_p (cm^3/g)**	**Weak (T<450 K)**	**Medium (T<600 K)**	**Strong (T>600 K)**	**Total acidity**	**Metal loading (%)**	**Particle size (nm)**	**Metal dispersion (%)**
Pt/Nb_2O_5	73.3	7.2	0.09	2.63	2.67	0.00	5.30	0.56	6.9	16.0
Pd/Nb_2O_5	92.3	6.2	0.15	1.82	2.72	0.00	4.54	0.59	5.2	44.8
Ni/Nb_2O_5	112.2	5.4	0.17	0.72	0.40	0.00	1.12	0.57	5.1	21.9
Pt/Al_2O_3	95.0	17.5	0.48	0.56	0.50	0.33	1.39	0.51	4.6	23.9
Pd/Al_2O_3	100.5	16.5	0.49	0.63	0.91	0.55	2.09	0.43	8.2	13.6
Ni/Al_2O_3	257.9	6.4	0.57	4.43	2.61	0.00	7.04	0.43	5.7	19.6

Six different molecules were detected, with a good correspondence between their m/z spectra (included in the Supplementary Information, Fig S2) and the sequential hydrogenation of the C15 adduct, as is shown in **Scheme 1**. Due to the instability of some of these intermediates as well as the isomerization among them, experimental results are grouped in four representative families of chemicals (Scheme 1). The first one (labelled as "A") involves all the isomers with one or both exocyclic C=C bonds hydrogenation. It is anticipated that the production of these two intermediates should be conditioned by the same types of parameters, which supports the combined analysis: optimum adsorption on the catalytic surface and activity limited only to metal particles, i.e., conditioned by metal dispersion, particle size and/or the intrinsic activity of each metal. The second one (labelled as "B") includes the intermediates to obtain the complete reduction of both furan cycles; this implies three main compounds, with an increasing amount of H_2, with m/z values from 246 to 250. The m/z 248 compound has one furan ring completely hydrogenated (THF cycle). The two intermediates with m/z 246 and 250 involve the

hydrogenation of the ketone group, because of the McLafferty rearrangement [36], since partial hydrogenation of a furan cycle is very unstable. Thus, these three compounds should require not the only metal activity but also a good acidity distribution of the catalytic support. The third one (labelled as C, m/z 252) corresponds to the derivate with all the C=C bonds hydrogenated, being considered as the final product since the total hydrogenated adduct (m/z 254) has not been produced in quantitative amounts. Again, the production of these adducts should be conditioned by properties related to the metals phase of the catalyst.

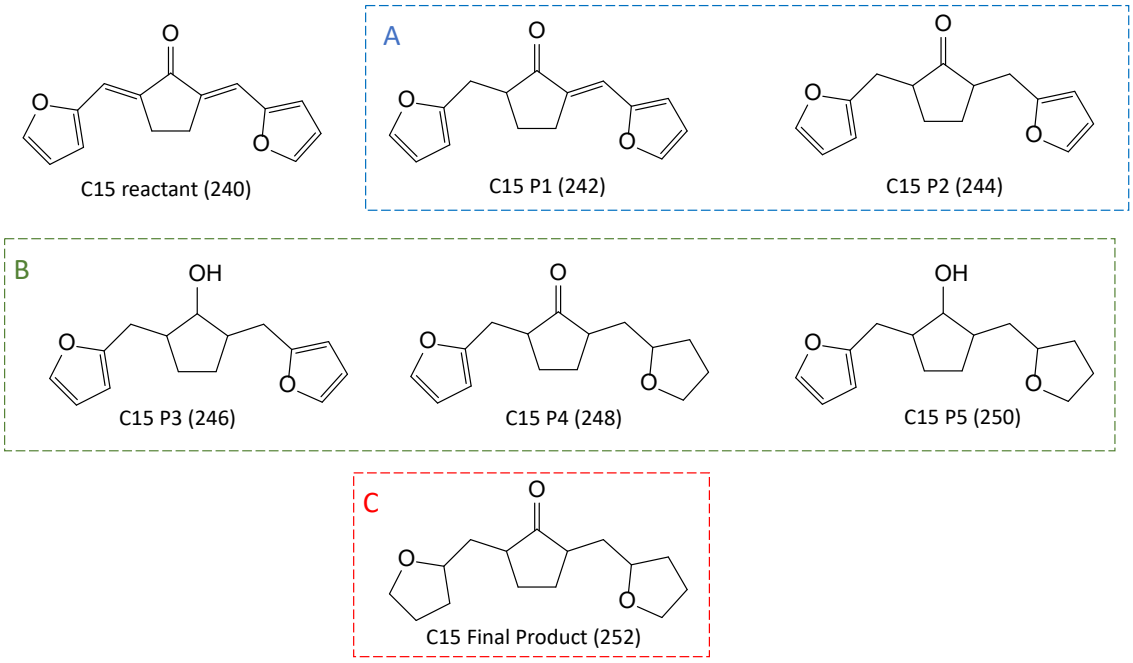

Scheme 1: Different compounds identified in the hydrogenation of cyclopentanone-furfural condensated product.

The distribution of all these compounds as a function of the catalyst after 8 h is plotted in **Figure 1**. In this figure, data related to C15 conversion and carbon balance are also added. The temporal evolution of each adduct, both in terms of concentration and yield, is included in the Supplementary Information (Fig. S3-S18). In general, terms, these results indicate a high prevalence of metal activity over the acid sites, suggesting the intrinsic catalytic properties of each metal as well as the metal dispersion as possible key parameters of this reaction.

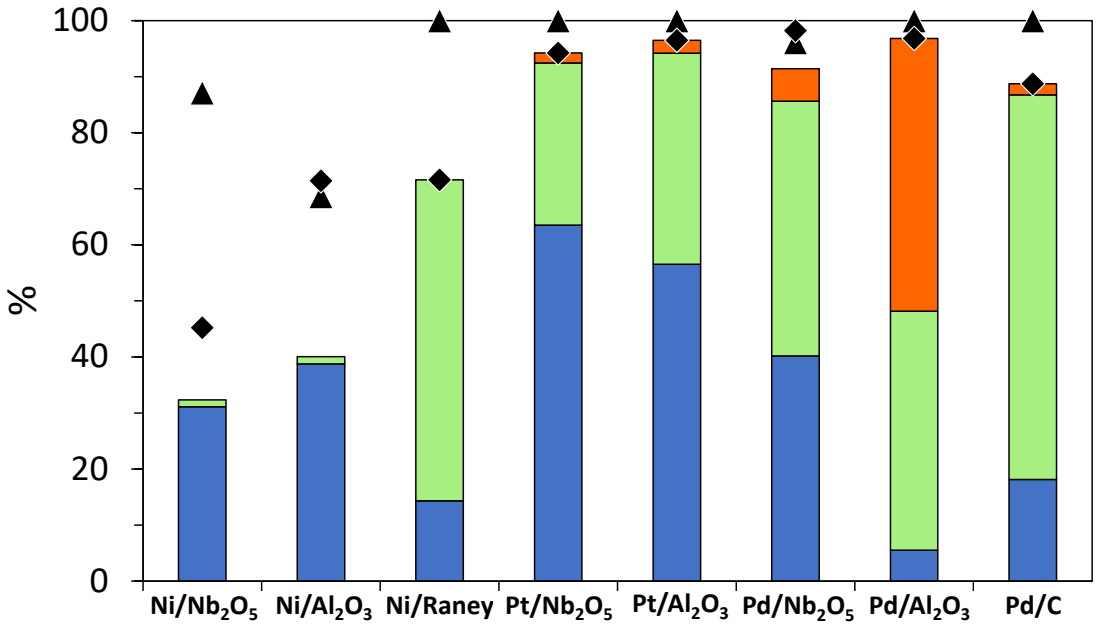

Figure 1: Comparison of main results obtained after 8 h of hydrogenation at 493 K as a function of the catalyst used. All the materials contain 0.5 % of metal loading. Results correspond to: (▲) conversion; (◆) carbon balance; A (blue); B (green); and C products

Ni-containing catalysts provide the lowest activities for both supports. In the case of the catalyst supported on Nb_2O_5, the almost total disappearance of the reactant is observed (conversion higher than 87 %). However, total yields lower than 35 % are quantified, with the main contribution of the first hydrogenated intermediate (P1, m/z 242, final yield of 29.7 %). Two main reasons can justify these results: (1) this catalyst enhances side reactions of C-C cleavage obtaining low-molecular-weight compounds, or (2) the catalyst-compounds affinity is so strong that desorption is not favoured. It could be assumed that degradation compounds would be detected by the GC-FID. As this is not the case, the first hypothesis is discarded. The second hypothesis is congruent with the lowest carbon balance closure obtained with this material (45 %).

As to the Ni/Al_2O_3, the carbon balance closure is significantly higher (71 %) but this value is conditioned by the decrease in the C15 conversion (68.6 %). Very similar yields are obtained, with only 39 % of the first family of intermediates (A) and less than 2 % of the second one. As in the case of Ni/Nb_2O_5, the first adduct (m/z 242) prevails over the second one (m/z 244), with a relative yield higher than 92 %. Similar results were obtained despite the support used, as well as the significant differences in acidity, which corroborates the lack of activity of this metal.

The high relevance of these adsorptions in comparison to results obtained with other catalysts (although the adsorption typically involves the catalytic support but not the specific metal nanoparticles) is explained by the co-presence of two reasons, with a synergetic effect: the high surface area (see **Table 1**) and the low activity of Ni nanoparticles. Adsorption is a surface process, being promoted by high surface areas, as in the case of these two materials. In addition, adsorption is mainly promoted by double bonds, and these unsaturations disappear as the reaction proceeds. Thus, the relevance of adsorption decreases as the hydrogenation activity increases. The low activity is also observed since the first intermediate, compound of molecular weight 242, included in the "A" family, is only clearly observed when using Ni materials (as it will be discussed below), whereas in the other cases the intermediate 244 is directly observed as the first compound obtained in the reaction.

An extra experiment using a commercial Ni-Raney catalyst has been carried out to discern if the poor results observed with these metals are conditioned by the low metal loading (0.5 % is a typical loading for noble metals but not for transition ones) or if they reveal a low catalytic activity of this metal. Results after 8 h indicate that, despite the large amount of Ni available, the target compound ("C") is not obtained, observing an enrichment in the intermediates with the C=C partially hydrogenated (57.3 % after 8 h of reaction). The low surface area of this material, 100 m^2/g according to the information given by the supplier (SigmaAldrich) is congruent with the lower relevance of adsorption processes, with a carbon balance closure of 71.6 %. These results support the initial hypothesis of low activity of Ni metal, despite the metal loading or support used. Thus, this metal is discarded for the following studies since it is not active enough to promote a good conversion, with only a partial hydrogenation capacity of the acyclic C=C and too strong adsorption.

In the case of the Pd- and Pt-containing catalysts, their highest activity minimized the effect of these adsorption processes, as concluded from the better carbon balance closures (94.2, 98.2, 96.5 and 96.8 %, with Pt/Nb_2O_5, Pd/Nb_2O_5, Pt/Al_2O_3 and Pd/Al_2O_3, respectively). In the four cases, the hydrogenated adduct is observed (product "C") with a clearly better behaviour of Pd catalysts.

In fact, the best results are obtained with Pd/Al_2O_3, with which the final product represents almost 50 % of the total yield (48.3 %). Pd is the most active metal, despite the support used, but a key role of alumina is also observed since the yield of product "C" is more than 8 times higher when this support is used. In the case of Pt, differences are less relevant; with fewer than 2.5 % of "C" product. In all these cases, the carbon balance closure is higher than 94 %, discarding relevant adsorption phenomena, and the C15 conversion is higher than 95 % (being 100 % in all the cases except Pd/Nb_2O_5).

Pd and Pt supported on alumina have the largest pore diameters (see Table 1), which could be presumed as the key parameter, considering the large size of molecules involved in this reaction. However, results obtained with Pd/Nb_2O_5 are significantly better than those with Pt/Al_2O_3, despite the smaller pore size. Thus, this assumption is discarded as the limiting parameter, although its positive relevance is assumed. All these results confirm that both catalytic phases (metal and acid support) are relevant in the activity. In fact, the presence of metal modifies the morphological and physic-chemical properties of the original materials, as it is summarized in Table 1. Although the bibliography demonstrate that, in general terms, acidity plays a positive role in hydrogenations [37,38], experimental data suggest that the effect is not globally positive, since all the results with alumina are better than the corresponding ones with niobium oxide, although the total acidity order is just the opposite. This unexpected behaviour has been previously observed in the hydrogenation of benzene, concluding that reaction is enhanced at low temperatures and with less acidic material, whereas side reactions grow progressively with the acid strength of the catalyst [39]. An alternative hypothesis to explain these results is that only the strong acidity is relevant in the process, considering that compounds P3 and P5 require the hydrogenation of cyclic unsaturations, which are significantly more stable than the acyclic ones. In good agreement with this, promising results are obtained with alumina supports since they have the strongest acid sites, but the prevalence of the metal activity disrupt the acidity order, observing more productivity with Pd/Nb_2O_5 than with Pt/Al_2O_3. Considering that both hypotheses could be complementary, a

synergetic effect is proposed, in which alumina is chosen as the best support, discarding the activity of Nb_2O_5 materials for further experiments, and Pd is identified as the most active metal.

An extra analysis with commercial Pd/C was carried out, results after 6 h being also included in Figure 1. Although complete conversion is also reached, the product distribution is significantly different, with only 2 % of the target product. The high surface area of this product (1690 m^2/g) [40] justifies the low carbon balance closure (88.7 %) in comparison to other Pd materials. However, this value is significantly higher than the ones obtained with Ni catalysts, in good agreement with the singular interaction Ni *vs.* compounds previously indicated. These results corroborate the synergetic effect of metal and support previously discussed.

The kinetic analysis (temporal evolution) could be very useful to go deeper into the metal and support influence. Despite the evolution of the different reaction products suggests a serial reaction [24,41], with consecutive hydrogenations, the evolution of selectivity as a function of the time predicts a more complex mechanism in which intermediates "A" and "B" can be also produced simultaneously (in the case of Pt/Al_2O_3), whereas compounds labelled with "C" (when observed) have clear final product progress, as it is shown in **Figure 2**. This general conclusion, however, must be disaggregated in particular analyses for each material, since the selectivity evolution as a function of the reactant conversion indicates three different situations for the three metals considered.

Thus, the first hydrogenation prevails in the case of the Pt catalysts, with initial selectivities to "A" family of intermediates close to 80 %, whereas there is 20 % of the "B" one. It can be concluded that both compounds could be detected at very low conversions, with a parallel behavior (and not the expected serial distribution). Concerning the "C" compounds, the results are not conclusive enough. It could be expected to be obtained from "B", but the profile of "B" has a continuous positive trend, even at 100 % conversion of the reactant, without observing any decrease. This result can be explained since, although "B" is consumed to produce "C", the global evolution is mainly affected by its formation from "A". An opposite situation is observed in the case of Pd, where the main compound detected at low conversions is the intermediate "B", with

selectivities close to 80 %. This result indicates that Pd is so active that the cyclic hydrogenation occurs at the same time as the hydrogenation of aliphatic unsaturations. With Pd, "C" is clearly obtained from "B", observing an almost total correspondence between the decrease in the "B" selectivity and the increase in the "C" one.

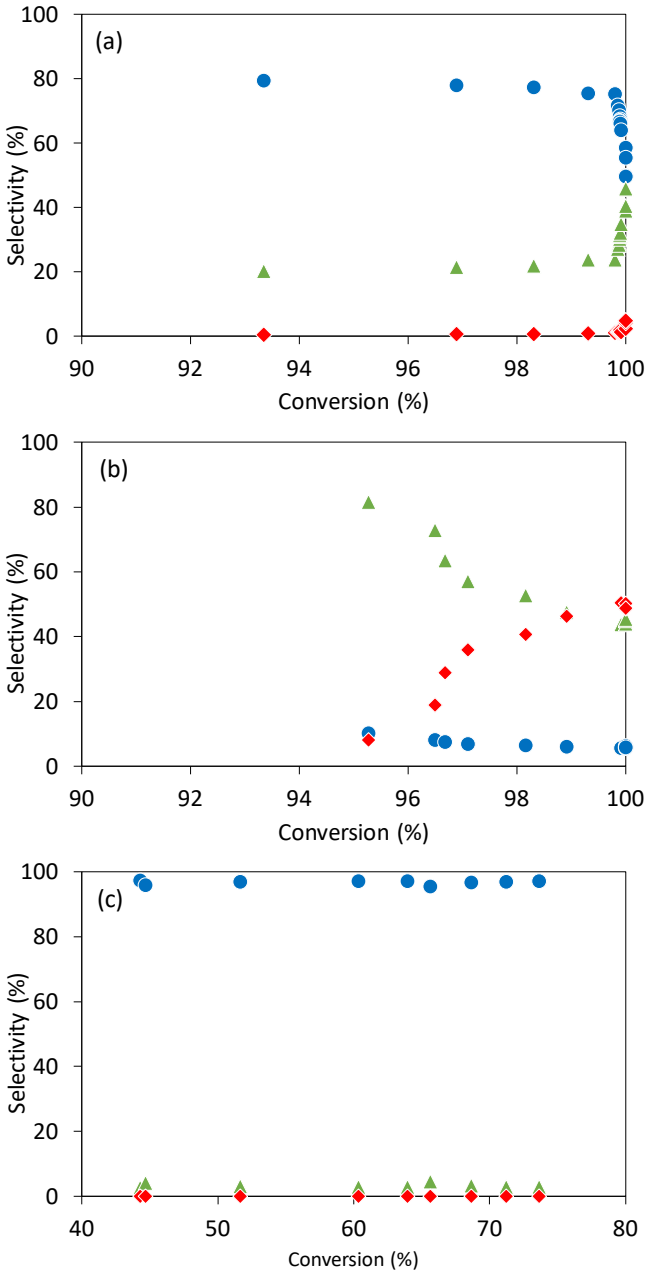

Figure 2: Evolution of selectivity to different intermediates identified in the C15 hydrogenation at 493 K as a function of the catalyst used (0.4 g/L of catalytic loading). Results correspond to (a) Pt/Al_2O_3; (b) Pd/Al_2O_3; (c) Ni/Al_2O_3. Symbols: (●) A; (▲) B; (◆) C.

Similar results were reported by Hronec *et al.,* observing that palladium was significantly more active for ring saturation than platinum or ruthenium [41]. In the case of Ni catalysts, intermediate A is the main compound detected despite the conversions, with almost negligible selectivity to B or C. These results suggest that Ni is not active enough to promote the subsequent steps of the hydrogenation. All these data can be fitted to the reaction mechanism illustrated in **Scheme 2**, corresponding to equations 1 to 4.

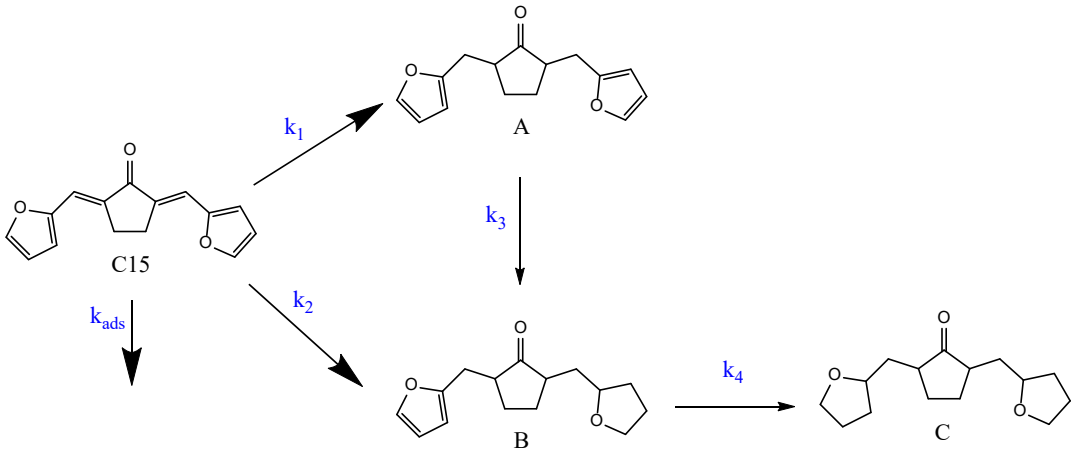

Scheme 2: Reaction mechanism proposed for the C15 hydrogenation.

$$\frac{d[C15]}{dt} = -k_1 \cdot [C15] - k_2 \cdot [C15] - k_{ads} \cdot [C15] \qquad [1]$$

$$\frac{d[A]}{dt} = k_1 \cdot [C15] - k_3 \cdot [A] \qquad [2]$$

$$\frac{d[B]}{dt} = k_2 \cdot [C15] + k_3 \cdot [A] - k_4 \cdot [B] \qquad [3]$$

$$\frac{d[C]}{dt} = k_4 \cdot [B] \qquad [4]$$

Experimental results were fitted considering these equations, in which first-order kinetic expressions are proposed. This assumption is congruent with previous literature concerning kinetic studies of similar compounds [19,42,43]. Langmuir-Hinshelwood kinetics do not provide an appropriate prediction of the reaction data, despite having a larger number of parameters than the proposed model. This fact suggests weak adsorption of the compounds involved, the kinetic

rates prevailing. The adjustment was solved using MATLAB code, performing all the calculations, and solving the set of ordinary differential equations ("ode45"). The fitting of the unknown parameters from the model is accomplished by the least-square method. The MATLAB function "lsqcurvefit" using the Levenberg-Marquardt algorithm was used. The coefficient of determination was calculated with the MATLAB function "rsquare". The kinetic constants values are summarized in **Table 2**, whereas the good adjustment among experimental and fitted values is observed in **Figure 3**.

Table 2: Summary of kinetic constants obtained fitting the experimental results obtained with different materials and the reaction mechanism proposed.

Catalyst	k_1 (min^{-1})	k_2 (min^{-1})	k_3 (min^{-1})	k_4 (min^{-1})	k_{ads} (min^{-1})
0.5 % Pt/Nb_2O_5	0.0671	0.0195	< 0.0001	0.0003	0.0036
0.5 % Pd/Nb_2O_5	0.0101	0.0207	0.0017	0.0126	0.0070
0.5 %Ni/Nb_2O_5	0.0027	0.0005	0.0012	<0.0001	0.0057
0.5 %Pt/Al_2O_3	0.0830	0.0206	0.0013	0.0010	0.0084
0.5 %Pd/Al_2O_3	0.0292	0.0312	0.0034	0.0024	0.0072
0.5 %Pd/Al_2O_3*	0.2160	0.2811	0.0366	0.0237	0.0613
0.5 % Ni/Al_2O_3	0.0126	0.0011	< 0.0001	0.0057	0.0019

*reaction using 1 g of catalyst.

As was expected, the differences observed in the evolution of selectivities are clearly observed in the relative weight of each step as a function of the catalyst used. Thus, values corresponding to Ni catalysts are the lowest obtained for almost all the steps. The low values obtained for the second kinetic constant indicates the prevalence of the metal activity since these catalysts cannot promote steps in which the acidity is partially involved, despite the higher acidity of these materials, in comparison to those of Pd or Pt. In good agreement with experimental results, the kinetic constants for the first step (k_1) reach the maximum value with Pt catalysts, whereas the good activity results of Pd ones is mainly justified by higher values of k_2 and k_3. Thus, this metal

promotes the hydrogenation of the cyclic hydrogenations, whereas Pt is active mainly for the exocyclic ones.

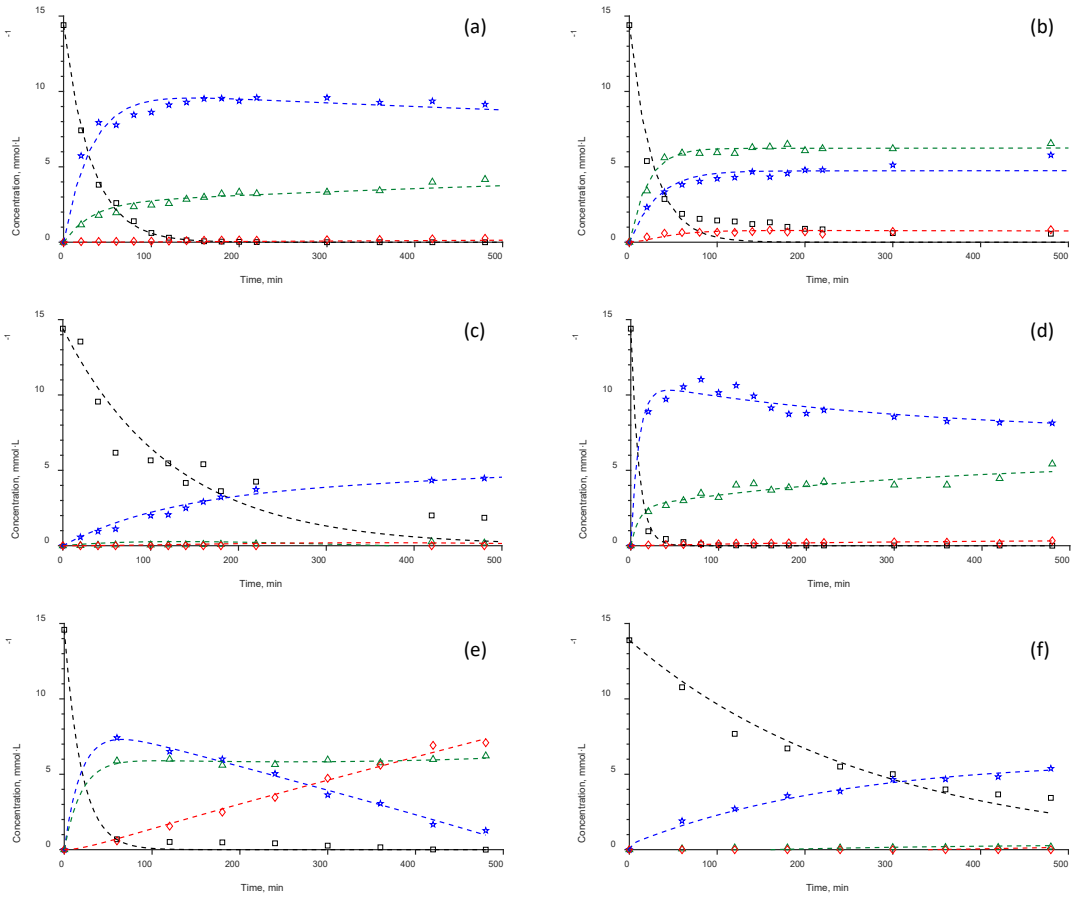

Figure 3: Comparison between experimental points (dots) and fitted values (broken lines). Results correspond to the C15 hydrogenation at 493K using a catalytic loading of 0.4 g/L. Data correspond to (a) Pt/Nb_2O_5; (b) Pd/Nb_2O_5; (c) Ni/Nb_2O_5; (d) Pt/Al_2O_3; (e) Pd/Al_2O_3; (f) Ni/Al_2O_3. Symbols: (⋆) A; (▲) B; (◆) C.

The positive role of Al_2O_3 is mainly observed in the case of Pd/Al_2O_3, with a specific effect in the first step of the reaction (from C15 to "A" intermediate) reaching kinetic values almost three times higher with this support than with the Nb_2O_5 (analysis corresponding to the k_1). This statement is not so evident with the other metals, suggesting a specific positive effect of this metal and support combination, promoting the optimum adsorption and interaction with the metal particle.

The lack of correspondence between these constants and the acidity or metal dispersion of these materials corroborates that hydrogenation of aromatic compounds does not depend on this property but on the intrinsic activity of each noble metal.

According to these results, Pd/Al_2O_3 is corroborated as the optimum catalyst for this reaction. The relatively low carbon balance observed with this material at intermediate times suggests that, despite the good results, adsorption is more relevant than in the previous cases. However, it is assumed that this adsorption is not permanent, and plays a positive role in the reaction, enhancing the interaction between reactant and the dissociated hydrogen. This analysis is because the amount of C obtained does not correspond to the disappearance of "A" or "B", the "A" concentration does not show the expected decreasing trend and the carbon balance increases as the reaction advances.

To check this hypothesis, the reaction has been carried out using 1 g of this catalyst (10 times higher than in the previous experiments). Results obtained after 8 h are compared in **Figure 4**, supporting the previous suggestion since the carbon balances increase, observing a relevant improvement in the final yield of product "C" (the complete hydrogenated one, 67.7 %), this value is more than 1.7 times higher than the previous one obtained with 0.1 g.

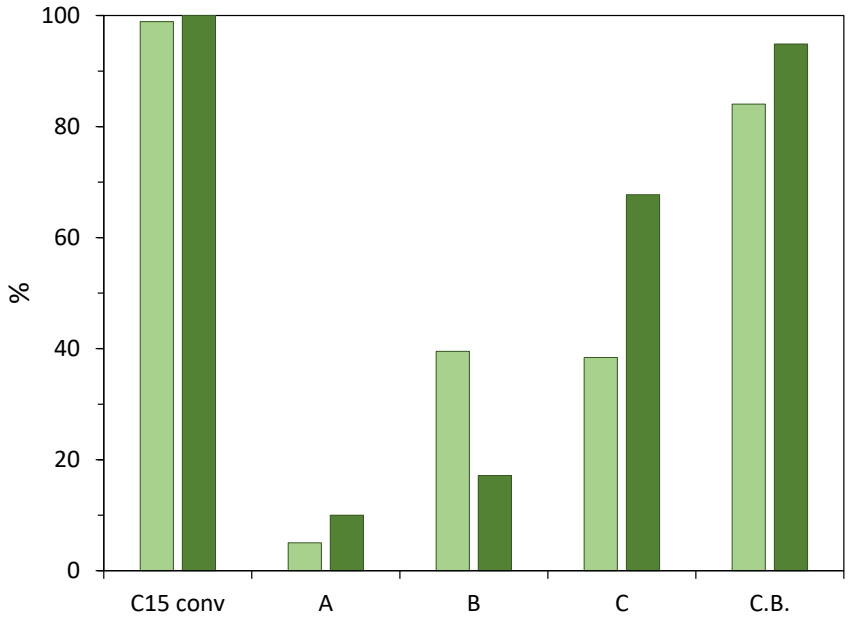

Figure 4: Comparison of results obtained after 8 h of hydrogenation at 493 K when using (light green) 0.1 g and (dark green) 1 g of 0.5 % Pd/Al_2O_3.

Results were fitted considering the previous kinetic model proposed. The kinetic constants are summarized in **Table 2**, being the goodness of this adjustment shown in **Figure 5**, in which the temporal evolution of results obtained with 1 g are shown, comparing experimental points (dots) with the fitted ones (lines).

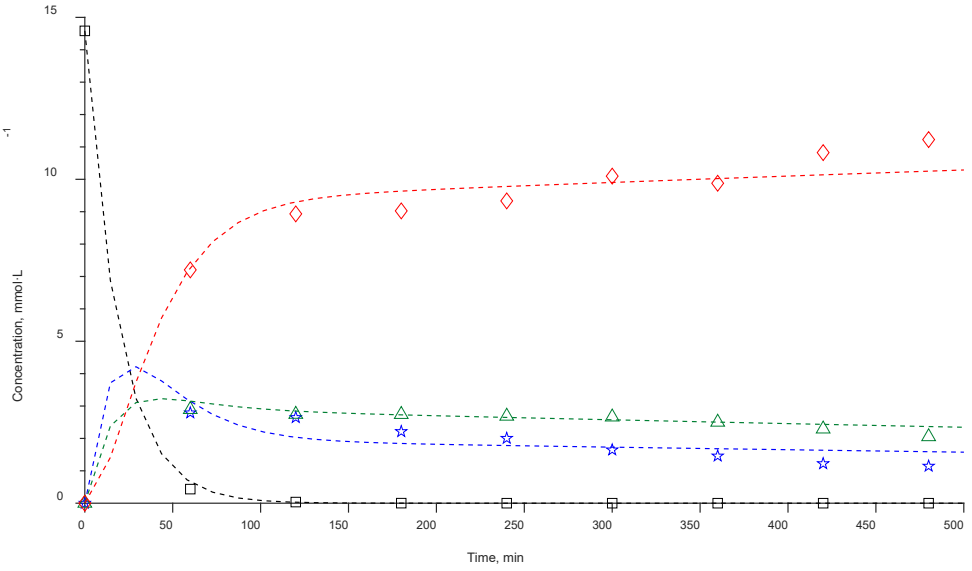

Figure 5. Comparison between experimental (dots) and fitted results (broken lines) in the hydrogenation of C15 adduct at 493 K with 1 g of 0.5 % Pd/Al_2O_3. Results correspond to (□) C15; (○) A; (Δ) B; and (◇) C.

The expected improvement because of having a ten times higher amount of catalyst is observed in the reactions involving the cyclic C=C bonds (mainly k_3 and k_4) whereas the influence in the first steps (k_1 and k_2) is less marked. In good agreement with the proportionality between the adsorption kinetic constant and the surface area, this value increases 2.3 times when using 1 g.

Effect of the solvent

The binary system ethanol-water initially was proposed to keep constant the system used for the previous condensation [10], being a starting point of a possible one-pot configuration and, then, reducing the costs of purification. However, it could affect catalyst activity due to the low aqueous-phase solubility of reactant and intermediates. Different strategies are analyzed to study

if working with a pure organic solvent the hydrogenation can be enhanced. It is already proved that organic solvents play an important role in the activity and selectivity of this type of reactions [24]. A solvent can produce fast solvation of the surface compounds, preventing its interaction with the catalytic surface [44,45]. On the other hand, the solvent can also influence the activation barrier, promoting interactions with the catalyst that can compete for the active sites [46,47]. Despite these general considerations, the influence of the reaction media (solvent) on the activity and selectivity in the hydrogenation of furfural-cyclopentanone condensation products has been scarcely discussed. The limited information available about the hydrogen solubility in different solvents is highlighted as the main cause of the absence of a clear discussion about that [21].

The possible influence of the organic solvent is compared in **Figure 6,** showing the main results obtained when using pure ethanol and butanol (protic polar solvents), acetone (aprotic polar solvent), and hexane and heptane (aprotic apolar solvents). The concentration and yield evolution of each reaction intermediate is included in the supplementary information (Fig. S19-S28). A fast comparison between results with the ethanol-water system and using only pure ethanol allows concluding that there is a clear improvement when water is removed from the system. These improvements are not only relevant in terms of activity and product distribution, but also in terms of carbon balance evolution during all the reaction. Thus, any permanent adsorption or undesired reaction disappears when using only organic solvents. In this case, the oligomerization is the main side reaction (due to the presence of a high amount of unsaturations). This oligomerization is promoted by the restricted solubility in water; a situation at which the compounds can be easily deposed or permanent adsorbed on the catalytic surface during times long enough to produce the oligomerization.

In general, the first hydrogenated adduct almost disappears when using only organic solvents, being only detected in the final mixture when using ethanol and acetone (yields of 5.4 and 5.5 %, respectively). With these solvents, the second intermediate (“B”) is the main product with 59 and 58.4 % yields, respectively. These results suggest that ethanol and acetone have similar behavior, different from the one obtained when using apolar solvents or heavier alcohol. In these three

cases, results after 6 h are very similar, with more than 70 % of the final yield of the total hydrogenated adduct ("C"). The best activity is observed with hexane, with 79 % of this compound with a final carbon balance of 98.7 %.

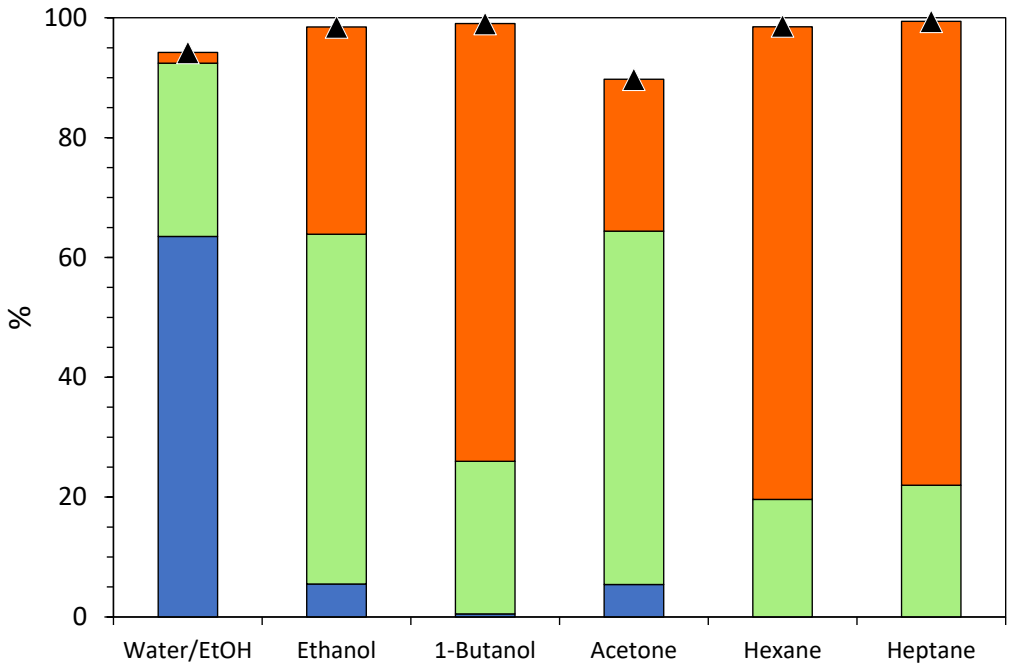

Figure 6: Comparison of main results obtained after 6 h of C15 hydrogenation at 493 K as a function of the solvent used and catalysed by 0.5 % Pd/Al_2O_3. Results correspond to total conversion of C15: (◆) carbon balance; A(blue); B(green); and C product (red).

Despite these similar results, a deeper study requires the analysis of selectivity distribution under iso-conversion conditions. This comparison is shown in **Figure 7,** plotting the results at 60 and 80 % of C15 conversion. As it was previously mentioned, the carbon balance is always higher than 93 % during all the reaction, in contrast with the values close to 70 % obtained with the mixture water:ethanol. According to these results, butanol is the most selective solvent, since the C component is obtained with yields higher than 60 % even when the C15 conversion is only 60 % (results corresponding to 36 min of reaction).

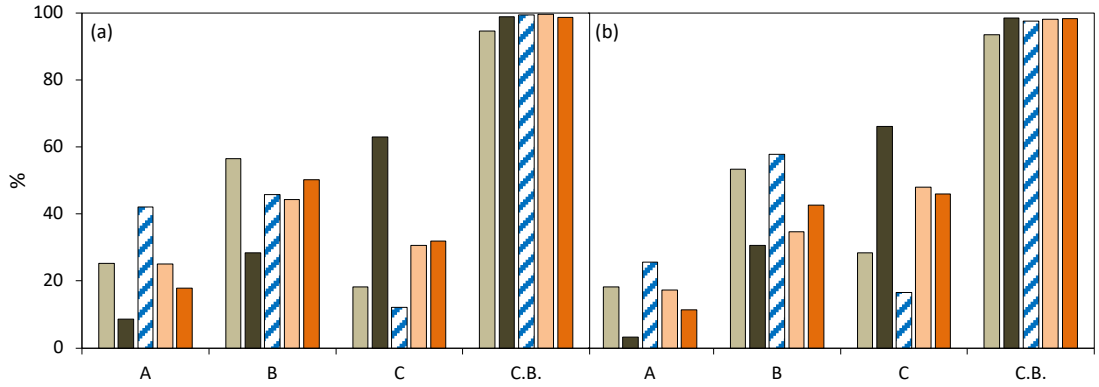

Figure 7: Comparison of main results of C15 hydrogenation (493 K) at the same conversion values (a) 60 % and (b) 80 %, catalyzed by 0.4 g/L of 0.5 % Pd/Al_2O_3. Results analysed as a function of the solvent: ethanol (light grey); 1-butanol (dark grey); acetone (blue lines); hexane (light orange) and heptane (dark orange). Results correspond to products yields and carbon balance closures.

All the solvents show a significant increase in the selectivity to "C" except the acetone, a solvent that has a very slight increase from results at 60 to 80 %. This fact suggests a higher difficulty to promote the last step of the reaction, "B" family of compounds being the main product detected. This effect, but less accused, is also observed with ethanol. There is not a clear correspondence between the molecular weight of the solvent and the activity, since trends obtained with ethanol and butanol are opposite to those obtained with hexane and heptane.

The temporal evolution of all the compounds involved in these reactions was analyzed as a function of the reaction mechanism previously proposed, obtaining a very good fitting (r^2>0.95 in all the cases), as shown in **Figure 8**, with the kinetic values summarized in **Table 3**. As was expected, kinetic constants are in almost all the cases, higher than those obtained with the binary mixture. This fact is more evident in the last steps of the reaction (k_3 and k_4).

Differences observed among the solvents used can be explained by different phenomena, highlighting: the interaction of the solvent with the reactant (solvation); the competitive adsorption (reactant *vs.* solvent) on the catalyst surface; and the solubility of hydrogen and reactants involved [21]. Hydrogen is more soluble in alkanes than in alcohols [48]. However, most of the authors agree that a clear correlation between hydrogenation activity and hydrogenation solubility cannot be established [49,50]. The effects related to the solubility of the reactants can be discarded since they were experimentally checked.

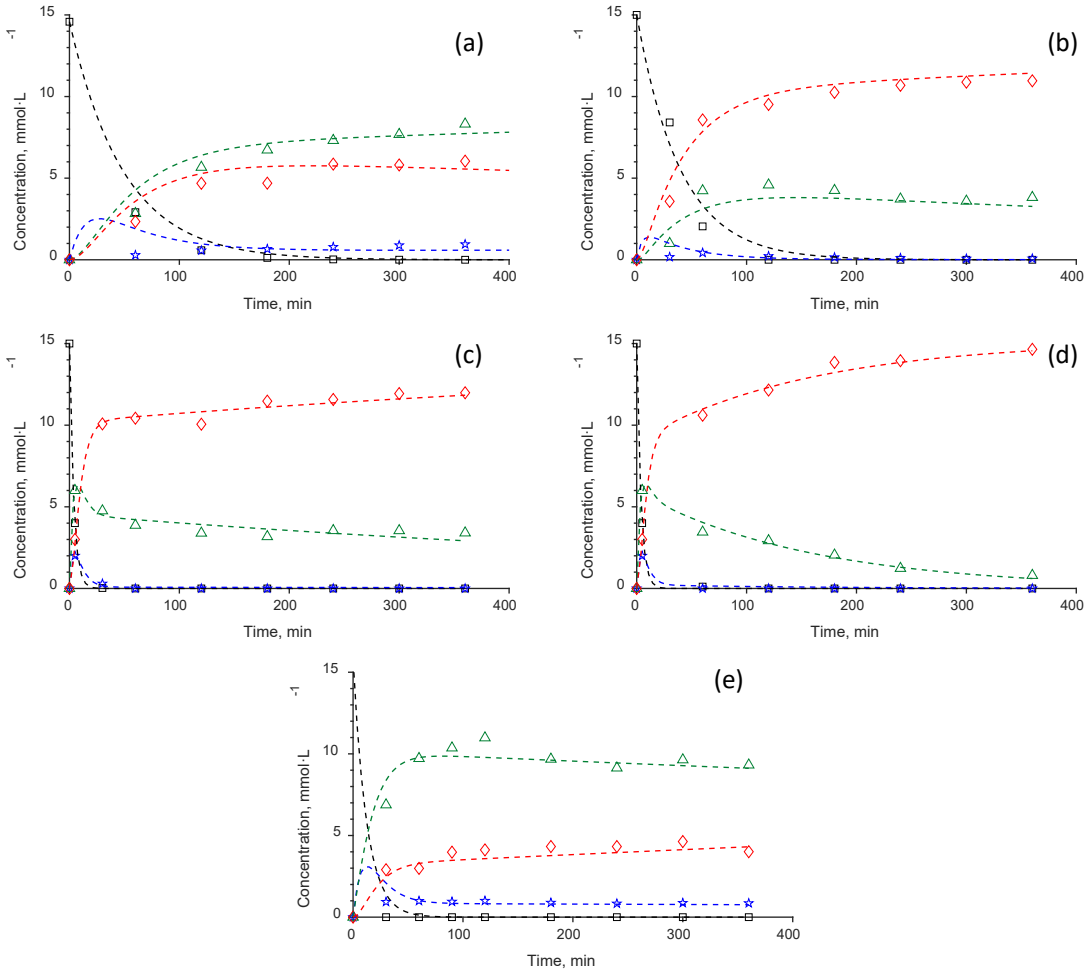

Figure 8: kinetic analysis of C15 hydrogenation at 493 K using 0.4 g/L of 0.5 % Pd/Al_2O_3. Comparison between experimental points (dots) and fitted values (broken lines). Results correspond to (a) ethanol; (b) 1-butanol; (c) hexane; (d) heptane; (e) acetone. Symbols: (●) A; (▲) B; (◆) C.

Table 3: Summary of kinetic constants obtained fitting the experimental results with different solvents and the reaction mechanism proposed. Dielectric constant (ε_r) and nucleophilic donor number (DN) of the different solvent are also included.

	ε_r	DN (kcal·mol^{-1})	k_1 (min^{-1})	k_2 (min^{-1})	k_3 (min^{-1})	k_4 (min^{-1})	k_{ads} (min^{-1})
Ethanol	24.6	32	0.0638	0.0193	0.0843	0.0038	0.0074
Butanol	17.8	29	0.0331	0.0085	0.1437	0.1415	0.0005
Acetone	21.01	17	0.0689	0.0099	0.0986	0.0027	0.0080
Hexane	1.89	0	0.0136	0.0216	0.0548	0.4180	0.0029
Heptane	1.92	0	0.0767	0.0840	0.0318	0.3845	0.0026

The poor results found with acetone can be explained by the formation of a strong complex between the aprotic polar solvent (electron-pair donor) and the metal phase (electron pair acceptor) [51]. This interaction produces competitive solvent-reactant adsorption since the solvent adsorbed is partially blocking the active sites, hindering the reaction. This is opposite to what happens with protic solvents, which promotes the interaction with the reactant (solvation), which also makes difficult the interaction reactant-metal site required for the hydrogenation [50, 52]. This effect increases with the polarity, explaining why butanol results are much better than the ethanol ones, according to the dielectric constant values. In addition, this effect is more evident in the kinetic constants of the advanced steps, since compounds including THF cycles are more polar than those including furan rings, enhancing the interaction with the solvent.

The good results obtained with hexane and heptane are explained because both negative effects, solvation, and competitive adsorption, are prevented when using apolar solvents, enhancing the required interaction between the reactant and the metal sites.

Globally, the best results are reached with butanol and hexane. At these conditions, the final mixture obtained has a cetane index of 26 (25.9 and 26.3, respectively). This value is calculated using the correlation proposed by Danaher and Johnston [53]. It implies 21 % more than the value obtained for the initial sample (condensated adduct). Considering that cetane indices for a commercial B20 are 45.3 and 46.7 [54], this mixture could be considered as a good fuel additive

that could be blended up to 42 % (w/w) with a pure pentadecane (the corresponding alkane in case of complete hydrodeoxygenation of the initial reactant).

Reusability

The catalytic reusability, together with the activity and selectivity, is one of the three requirements for the scaling-up of the catalytic process. To check the possible reusability of Pd/Al_2O_3, the spent catalyst was recovered by filtration after the reaction cycle and reused again after being dried overnight at 378 K, without any regeneration process between cycles. Considering the activity results, the stability was studied in parallel considering the butanol and hexane as solvents. Results after 6 h are compared in **Figure 9**.

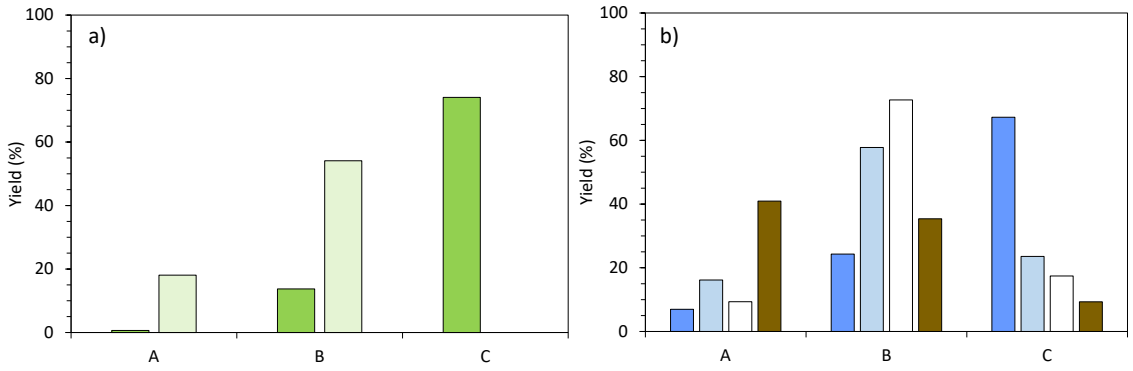

Figure 9: Pd/Al_2O_3 reusability results. Analysis for the C15 hydrogenation at 493 K as a function of the solvent used. Data correspond to (a) butanol and (b) hexane solvents. Dark green and blue bars correspond to the first cycle, light colors correspond to the second one and white indicates the third cycle. A four-cycle after regeneration is shown in gold color.

Concerning the experiments using butanol as a solvent, total C15 conversion is reached in the second cycle but the hydrogenated adduct totally disappears, with a yield distribution of 18 % and 54 % of the first and second adduct, respectively. The significant decrease in the carbon balance closure (from 88.4 to 72.2 %) suggests a relevant influence of the adsorption process, maybe stabilized by the polar character of this solvent. Thus, this catalyst was discarded for a third cycle, considering that the reusability without regeneration is not a good option for this approach.

As to the reactions using hexane, results indicate higher stability, observing the target product during the first three cycles. A total conversion is reached in all the cases, with a decrease in the activity for the last step of the process, obtaining a higher yield of the partially hydrogenated compound ("B" intermediates) because of the decrease in the target compound: from 24 to 58 % in case of "B" yield; from 67 to 25 % in case of "C" one. A more stable situation is observed comparing the second with the third cycle, with more than 18 % of "C" in the liquid mixture after 6 h of reaction, which means a reduction lower than 30 %. This deactivation is mainly affecting the last step of the process, whereas the conversion and carbon balance closure do not suffer any alteration, obtaining final samples enriched in the "B" intermediates. These results suggest that possible oligomers are stably adsorbed on the metal nanoparticles, preventing the hydrogenation of the most stable unsaturation.

In order to check this hypothesis, the spent catalysts after two cycles with butanol and after one cycle with hexane were recovered by filtration, dried in an oven at 100ºC and their carbonaceous deposits decomposition into CO_2 was measured by the temperature-programmed oxidation (TPO). Results obtained are compared in Figure 10. Signal obtained after the reaction in butanol (red line) only shows a peak, with a maximum desorption temperature of 580 K. The intensity of this peak is significantly lower than the corresponding ones of catalyst used in hexane (650, 740 and 815 ºC), indicated by the black line, and the oxidation temperature is significantly lower, suggesting a different type of deposit. This result seems to be opposite to the highest deactivation observed with butanol, in comparison to the cycle with hexane. It is suggested that the deposits produced with the butanol are due to organic compounds permanent adsorbed on the metal particles, preventing their role in hydrogenation by poisoning. On the other hand, the deposits observed in presence of butanol could be mainly affecting the alumina surface, producing a slower deactivation by fouling.

With the aim to try to recover the catalytic activity, the catalyst recuperated after three cycles in hexane was regenerated by thermal treatment (823 K 12 h) and reduced following the same procedure as for fresh materials. This temperature is chosen based on the oxidation temperatures

observed in the TPOs and it is in good agreement with the maximum temperature reached during the preparation procedure. The good regeneration was analyzed by TPO without observing any signal related to the remaining organic deposits in the fresh regenerated material. However, the desired reactivation is not observed, reaching a final mixture enriched in the first two families of compounds: “A” and “B”. The TPO analysis of the spent material (broken line in Figure 10), indicates the appearance, with significant relevance, of a first peak at low temperature (610 K). This peak (similar to the one observed in butanol) could correspond to deposits on the metal phase, justifying the high decrease in the hydrogenation activity. The high relevance of this peak after the regeneration step could be justified by a metal sintering produced by the thermal treatment (the initial metal dispersion of this material was not very high), concluding that a total regeneration by a thermal procedure is not possible due to the discrepancies between the energy required to oxidize the organic deposits and the metal stability.

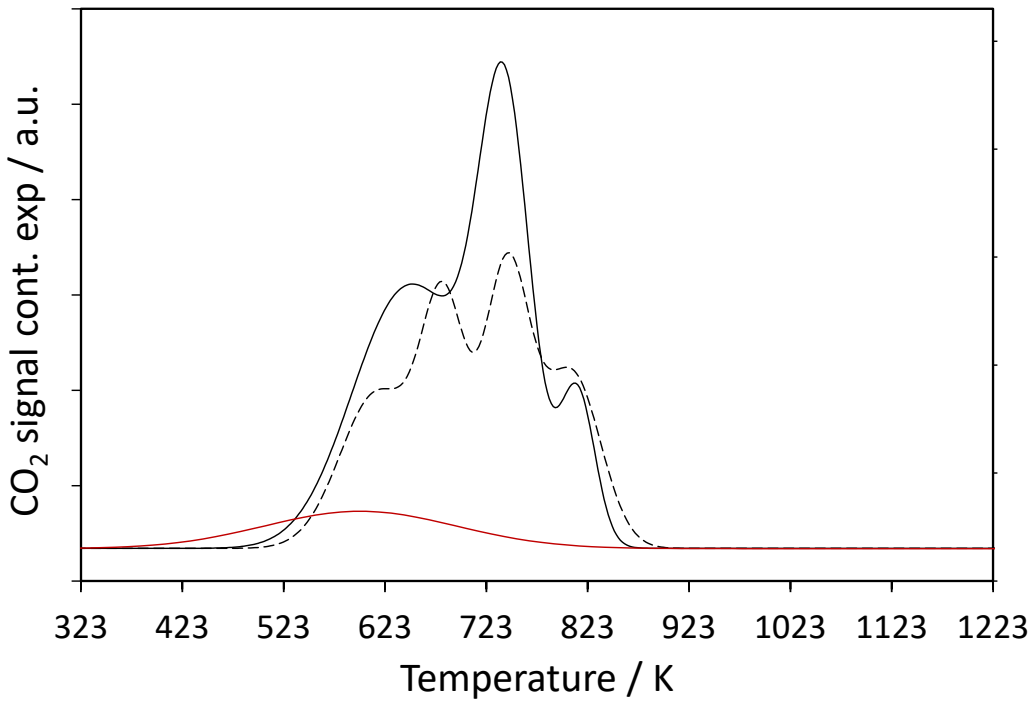

Figure 10: TPO analysis of spent catalysts. Results corresponding to the second cycle with butanol (red line), the first cycle with hexane (black one) and the regenerated catalyst after a reaction cycle (broken lines)

CONCLUSIONS

The hydrogenation of C15 has been studied considering different metals and supports It was concluded that the requirement of both, cyclic and acyclic C=C bonds hydrogenation discard the activity of Ni, mainly obtaining the first adduct. The great activity of 0.5 %Pd/Al_2O_3 suggests a synergetic effect of this metal and the support, combined with the optimum distribution of acidity.

This yield is strongly increased (up to 75 %) when removing water for the reaction system, using hexane or butanol as solvents. Results obtained with different solvents are discussed as a function of the kinetic and their physical properties, concluding that a good solvent must prevent the competitive adsorption reactant vs. solvent on the catalytic surface (discarding the use of acetone) and reduce the solvation by using solvents with low dielectric constants. The goodness of these results is tested as a function of the cetane index, obtaining a final mixture that could be blended up to 48 % with pure alkane to obtain an optimum diesel fuel.

ACKNOWLEDGEMENTS

This work has been financed by the Spanish Ministry of Economy and Competitiveness (CTQ2017-89443-C3-2-R).

REFERENCES

[1] Baloch, H.A., Nizamuddin, S., Siddiqui, M.T., Riaz, S., Jatoi, A.S., Dumbre, D.K., Mubarak, N.M., Srinivasan, M.P., Griffin, G.J., Recent advances in production and upgrading of bio-oil from biomass: a critical overview. J. Env. Chem. Eng., 6 (2018) 5101-5118. https://doi.org/j.jece.2018.07.050.

[2] Chato, R.J.A., Cuevas, C.C.R., Tangpuz, J.S.N., Cabatingan, L.K., Go, A.W., Ju, Y.H., Dilute acid hydrolysis as a method of producing sugar-rich hydrolysates and lipid-dense cake residues from copra cake. J. Env. Chem. Eng., 6 (2018) 5693-3705. https://doi.org./j.jece.2018.08.072.

[3] M.Z. Li, J.N. Wei, G.H. Yan, H. Liu, X. Tang, Y. Sun, X.H. Zeng, T.Z. Lei, L. Lin, *Cascade conversion of furfural to fuel bioadditive ethyl levulinate over bifunctional zirconium-*

based catalysts, Renew. Energ. 147 (2020) 916-923. https://doi.org/10.1016/j.renene.2019.09.064.

[4] J. Ma, S. Shi, X. Jia, F. Xia, H. Ma, J. Gao, J. Xu, *Advances in catalytic conversion of lignocellulose to chemicals and liquid fuels*, J. Energy Chem. 36 (2019) 74-86. https://doi.org/10.1016/j.jechem.2019.04.026.

[5] H. Zhang, M. Han, C. Yang, L. Yu, Q. Xu, *Gram-scale preparation of dialkylideneacetones through Ca (OH) 2-catalyzed Claisen-Schmidt condensation in dilute aqueous EtOH.* Chinese Chem. Lett. 30 (2019), 263-265. https://doi.org/10.1016/j.cclet.2018.01.035.

[6] A.S. Amarasekara, C.D.G. Reyes, *Bronsted acidic ionic liquid catalysed one-pot conversion of cellulose to furanic biocrude and identification of the products using LC-MS*, Renew. Energ. 136 (2019) 352-357. https://doi.org/10.1016/j.renene.2018.12.108.

[7] Y. Nakagawa, M. Tamura, K. Tomishige, *Recent development of production technology of diesel-and jet-fuel-range hydrocarbons from inedible biomass*. Fuel Process. Technol. 193 (2019), 404-422. https://doi.org/10.1016/j.fuproc.2019.05.028.

[8] J. Cueto, L. Faba, E. Díaz, S. Ordóñez, *Cyclopentanone as an alternative linking reactant for heterogeneously catalyzed furfural aldol condensation*, ChemCatChem 9 (2017) 1765-1770. https://doi.org/10.1002/cctc.201601655.

[9] S. Dutta, B. Saha, *Hydrodeoxygenation of furylmethane oxygenates to jet and diesel range fuels: probing the reaction network with supported palladium catalyst and hafnium triflate promoter*, ACS Catal. 7 (2017) 5491-5499. https://doi.org/10.1021/acscatal.7b00986.

[10] J. Cueto, L. Faba, E. Díaz, S. Ordóñez, *Enhancement of furfural–cyclopentanone aldol condensation using binary water–ethanol mixtures as solvent,* J. Chem. Technol. Biotechnol. 93 (2018) 1563-1571. https://doi.org/10.1002/jctb.5522.

[11] L. Faba, E. Díaz, S. Ordóñez, *One-pot Aldol Condensation and Hydrodeoxygenation of Biomass-derived Carbonyl Compounds for Biodiesel Synthesis*, ChemSusChem 7 (2014) 2816-2820. https://doi.org/10.1002/cssc.201402236.

[12] A. Bohre, B. Saha, M.M. Abu Omar, *Catalytic upgrading of 5-hydroxymethylfurfural to drop-in biofuels by solid base and bifunctional metal–acid catalysts*, ChemSusChem 8 (2015) 4022-4029. https://doi.org/10.1002/cssc.201501136.

[13] O. Kikhtyanin, R. Bulánek, K. Frolich, J. Čejka, D. Kubička, *Aldol condensation of furfural with acetone over ion-exchanged and impregnated potassium BEA zeolites*, J. Mol. Catal. Chem. 424 (2016) 358-368. https://doi.org/10.1016/j.molcata.2016.09.014.

[14] R.S. Malkar, H. Daly, C. Hardacre, G.D. Yadav, *Aldol condensation of 5-hydroxymethylfurfural to fuel precursor over novel aluminum exchanged-DTP@ ZIF-8*, ACS Sust. Chem. Eng. 7 (2019) 16215-16224. https://doi.org/10.1021/acssuschemeng.9b02939.

[15] O. Kikhtyanin, Y. Ganjkhanlou, D. Kubička, R. Bulánek, J. Čejka, *Characterization of potassium-modified FAU zeolites and their performance in aldol condensation of furfural and acetone*, Appl. Catal. A 549 (2018) 8-18. https://doi.org/10.1016/j.apcata.2017.09.017.

[16] G. R. Hafenstine, K. Ma, A. W. Harris, O. Yehezkeli, E. Park, D. W. Domaille, A. P. Goodwin, *Multicatalytic, light-driven upgrading of butanol to 2-ethylhexenal and hydrogen under mild aqueous conditions*, ACS Catal. 7 (2017), 568-572. https://doi.org/10.1021/acscatal.6b03213.

[17] Y. Nakagawa, S. Liu, M. Tamura, K. Tomishige, *Catalytic total hydrodeoxygenation of biomass-derived polyfunctionalized substrates to alkanes*, ChemSusChem 8 (2015) 1114-1132. https://doi.org/10.1002/cssc.201403330.

[18] A.D. Sutton, F.D. Waldie, R. Wu, M. Schlaf, A. Louis III, J.C. Gordon, *The hydrodeoxygenation of bioderived furans into alkanes*, Nat. Chem. 5 (2013) 428. https://doi.org/10.1038/nchem.1609.

[19] L. Faba, E. Díaz, S. Ordóñez, *Hydrodeoxygenation of acetone–furfural condensation adducts over alumina-supported noble metal catalysts*, Appl. Catal. B 160-161 (2014) 436-444. https://doi.org/10.1016/j.apcatb.2014.05.053.

[20] B. Yoosuk, P. Sanggam, S. Wiengket, P. Prasassarakich, *Hydrodeoxygenation of oleic acid and palmitic acid to hydrocarbon-like biofuel over unsupported Ni-Mo and Co-Mo sulphide catalysts.* Renew. Energ. 139 (2019) 1391-1399. https://doi.org/10.1016/j.renene.2019.03.030.

[21] R. Ramos, Z. Tišler, O. Kikhtyanin, D. Kubička, *Solvent effects in hydrodeoxygenation of furfural-acetone aldol condensation products over Pt/TiO_2 catalyst*, Appl. Catal. A 530 (2017) 174-183. https://doi.org/10.1016/j.apcata.2016.11.023.

[22] Le-Phu, N., Ngo, P.T., Ha, Q.L.M., Tran, T.V., Phan, T.T., Luu, L.C., Duong, L.T., Phan, B.M.Q., Efficient hydrodeoxygenation of guaiacol and fast-pyrolysis in oil from rice straw over PtNiMo/SBA-15 catalyst fro co-processing in fluid catalytic cracking process. J. Env. Chem. Eng., 8 (2020) 103552. https://doi.org/10.1016/j.jece.2019.103552.

[23] J.F. Feng, Z.Z. Yang, C.Y. Hse, Q.L. Su, K. Wang, J.C. Jiang, J.M. Xu, *In situ hydrogenation of model compounds and biomass-derived phenolic compounds for bio-oil upgrading.* Renew. Energ. 105 (2017) 140-148. https://doi.org/10.1016/j.renen.2016.12.054.

[24] M. Hronec, K. Fulajtárová, T. Liptaj, T. Soták, N. Prónayová, *Nickel catalysed hydrogenation of aldol condensation product of furfural with cyclopentanone to C15 cyclic ethers,* Chemistry Select 1 (2016) 331-336. https://doi.org/10.1002/slct.201500001.

[25] M. Balakrishnan, E. R. Sacia, A. T. Bell, *Selective hydrogenation of furan-containing condensation products as a source of biomass-derived diesel additives,* ChemSusChem 7 (2014) 2796-2800. https://doi.org/10.1002/cssc.201402764.

[26] S. Li, B. Liu, J. Truong, Z. Luo, P. C. Ford, M. M. Abu-Omar, *One-pot hydrodeoxygenation (HDO) of lignin monomers to C9 hydrocarbons co-catalysed by Ru/C and Nb_2O_5*. Green Chem 22 (2020), 7406-7416. https://doi.org/10.1039/D0GC01692F.

[27] Y. Nakagawa, K. Takada, M. Tamura, K. Tomishige, *Total hydrogenation of furfural and 5-hydroxymethylfurfural over supported Pd–Ir alloy catalyst.* ACS Catal. 4 (2014), 2718-2726. https://doi.org/10.1021/cs500620b

[28] Y. Nakagawa, M. Tamura, K. Tomishige*, Supported metal catalysts for total hydrogenation of furfural and 5-hydroxymethylfurfural*. J. Jpn. Petrol. Inst. 60 (2017) 1-9. https://doi.org/10.1627/jpi.60.1

[29] J.C. Serrano-Ruiz, J.A. Dumesic, *Catalytic Processing of Lactic Acid over Pt/Nb_2O_5*, ChemSusChem 2 (2009) 581-586. https://doi.org/10.1002/cssc.200900004.

[30] S. Chen, G. Zhou, H. Xie, Z. Jiao, X. Zhang, *Hydrodeoxygenation of methyl laurate over the sulfur-free Ni/γ-Al_2O_3 catalysts,* Appl. Catal. A 569 (2019) 35-44. https://doi.org/10.1016/j.apcata.2018.10.014.

[31] X. Kong, W. Lai, J. Tian, Y. Li, X. Yan, L. Chen, *Efficient Hydrodeoxygenation of Aliphatic Ketones over an Alkali-Treated Ni/HZSM-5 Catalyst*, ChemCatChem 5 (2013) 2009-2014. https://doi.org/10.1002/cctc.201200824.

[32] L.F.d. Sousa, F.S. Toniolo, S.M. Landi, M. Schmal, *Investigation of structures and metallic environment of the Ni/Nb_2O_5 by different in situ treatments – Effect on the partial oxidation of methane,* Appl. Catal. A 537 (2017) 100-110. https://doi.org/10.1016/j.apcata.2017.03.015.

[33] J. T. Scanlon, D. E. Willis, *Calculation of flame ionization detector relative response factors using the effective carbon number concept.* J Chromatogr Sci 23 (1985) 333-340. https://doi.org/10.1093/chromsci/23.8.333.

[34] T. Prapasawat, M. Hronec, M. Štolcová, A.W. Lothongkum, U. Pancharoen, S. Phatanasri, *Thermodynamic models for determination of the solubility of 2,5-bis(2-furylmethylidene)cyclopentan-1-one in different solvents at temperatures ranging from 308.15 to 403.15K*, Fluid Ph. Equilibria 367 (2014) 57-62. https://doi.org/10.1016/j.fluid.2014.01.039.

[35] L. Faba, E. Díaz, S. Ordóñez, *Role of the support on the performance and stability of Pt-based catalysts for furfural–acetone adduct hydrodeoxygenation*, Catal. Sci. Technol. 5 (2015) 1473-1484. https://doi.org/10.1039/C4CY01360C.

[36] P. R. Briggs, T. W. Shannon, P. Vouros, *Hydrogen exchange in a six-membered ring transition state. Evidence for a stepwise McLafferty rearrangement*. Organic Mass Spectrometry, 5 (1971) 545-550. https://doi.org/10.1002/oms.1210050506.

[37] S.G.A. Ferraz, B.M. Santos, F.M.Z. Zotin, L.R.R. Araujo, J.L. Zotin, *Influence of support acidity of NiMo sulfide catalysts for hydrogenation and hydrocracking of tetralin and its*

reaction intermediates, Industrial & Engineering Chemistry Research 54 (2015) 2646-2656. https://doi.org/10.1021/ie504545p.

[38] S. Handjani, E. Marceau, J. Blanchard, J.-M. Krafft, M. Che, P. Mäki-Arvela, N. Kumar, J. Wärnå, D.Y. Murzin, *Influence of the support composition and acidity on the catalytic properties of mesoporous SBA-15, Al-SBA-15, and Al_2O_3-supported Pt catalysts for cinnamaldehyde hydrogenation,* J. Catal. 282 (2011) 228-236. https://doi.org/10.1016/j.jcat.2011.06.017.

[39] O. Cairon, K. Thomas, A. Chambellan, T. Chevreau, *Acid-catalysed benzene hydroconversion using various zeolites: Brönsted acidity, hydrogenation and side-reactions*, Appl. Catal. A 238 (2003) 167-183. https://doi.org/10.1016/S0926-860X(02)00338-1.

[40] E. Díaz, L. Faba, S. Ordóñez, *Effect of carbonaceous supports on the Pd-catalyzed aqueous-phase trichloroethylene hydrodechlorination*. Appl Catal B-Environ 104 (2011) 415-417. https://doi.org/10.1016/j.apcatb.2011.03.031.

[41] M. Hronec, K. Fulajtárova, T. Liptaj, N. Prónayová, T. Soták, *Bio-derived fuel additives from furfural and cyclopentanone*, Fuel Processing Technology 138 (2015) 564-569. https://doi.org/10.1016/j.fuproc.2015.06.036

[42] G. Singh, L. Singh, J. Gahtori, R. K. Gupta, C. Samanta, R. Bal, A. Bordoloi, Catalytic hydrogenation of furfural to furfuryl alcohol over chromium-free catalyst: Enhanced selectivity in the presence of solvent. Molecular Catalysis 500 (2021) 111339. https://doi.org/10.1016/j.mcat.2020.111339

[43] J. Gu, J. Zhang, Y. Wang, D. Li, H. Huang, H. Yuan, Y. Chen, Efficient transfer hydrogenation of biomass derived furfural and levulinic acid via magnetic zirconium nanoparticles: Experimental and kinetic study. Industrial Crops and Products 145 (2020) 112133. https://doi.org/10.1016/j.indcrop.2020.112133

[44] S.H. Mushrif, S. Caratzoulas, D.G. Vlachos, *Understanding solvent effects in the selective conversion of fructose to 5-hydroxymethyl-furfural: a molecular dynamics investigation*, Phys. Chem. Chem. Phys. 14 (2012) 2637-2644. https://doi.org/10.1039/C2CP22694D.

[45] V. Vasudevan, S.H. Mushrif, *Insights into the solvation of glucose in water, dimethyl sulfoxide (DMSO), tetrahydrofuran (THF) and N, N-dimethylformamide (DMF) and its possible implications on the conversion of glucose to platform chemicals*, Rsc Adv. 5 (2015) 20756-20763. https://doi.org/10.1039/C4RA15123B.

[46] S.H. Mushrif, J.J. Varghese, C.B. Krishnamurthy, *Solvation dynamics and energetics of intramolecular hydride transfer reactions in biomass conversion*, Phys. Chem. Chem. Phys. 17 (2015) 4961-4969. https://doi.org/10.1039/c4cp05063k.

[47] M.A. Mellmer, C. Sener, J.M.R. Gallo, J.S. Luterbacher, D.M. Alonso, J.A. Dumesic, *Solvent effects in acid-catalyzed biomass conversion reactions,* Angew. Chem. 53 (2014) 11872-11875. https://doi.org/10.1002/anie.201408359.

[48] T.K.H. Trinh, J.C. de Hemptinne, R. Lugo, N. Ferrando, J.P. Passarello, *Hydrogen solubility in hydrocarbon and oxygenated organic compounds,* J. Chem. Eng. Data 61 (2016) 19-34. https://doi.org/10.1021/acs.jced.5b00119.

[49] E. Toukoniitty, P. Mäki-Arvela, J. Kuusisto, V. Nieminen, J. Päivärinta, M. Hotokka, T. Salmi, D.Y. Murzin, *Solvent effects in enantioselective hydrogenation of 1-phenyl-1,2-propanedione,* J. Mol. Catal. A 192 (2003) 135-151. https://doi.org/10.1016/S1381-1169(02)00415-6.

[50] N.M. Bertero, A.F. Trasarti, C.R. Apesteguía, A.J. Marchi, *Solvent effect in the liquid-phase hydrogenation of acetophenone over Ni/SiO_2: A comprehensive study of the phenomenon*, Appl.Catal. A 394 (2011) 228-238. https://doi.org/10.1016/j.apcata.2011.01.003.

[51] C. Reichardt, T. Welton, *Solvents and solvent effects in organic chemistry*, John Wiley & Sons, Germany, 2011. ISBN: 3527642137.

[52] J. He, C. Zhao, J.A. Lercher, *Impact of solvent for individual steps of phenol hydrodeoxygenation with Pd/C and HZSM-5 as catalysts*, J. Catal. 309 (2014) 362-375. https://doi.org/10.1016/j.jcat.2013.09.009.

[53] W.J. Danaher, P.A. Johnston, *The dependence on chemical composition of the cetane quality of hydrotreated light cycle oil*, Fuel Sci. Technol. Int. 5 (1987) 499-511. https://doi.org/10.1080/08843758708915862.

[54] N. Bezaire, K. Wadumesthrige, K.Y. Simon Ng, S.O. Salley, *Limitations of the use of cetane index for alternative compression ignition engine fuels*, Fuel 89 (2010) 3807-3813. https://doi.org/10.1016/j.fuel.2010.07.013.